Development Approach and Status of the 12.5 kW HERMeS Hall Thruster for the Solar Electric Propulsion Technology Demonstration Mission

IEPC-2015-186／ISTS-2015-b-186

Presented at Joint Conference of 30th International Symposium on Space Technology and Science
34th International Electric Propulsion Conference and 6th Nano-satellite Symposium,
Kobe, Hyogo, Japan
July 4 – 10, 2015

Richard Hofer[1*], Hani Kamhawi[2†], Daniel Herman[2‡], James Polk[1§], John Steven Snyder[1**], Ioannis Mikellides[1††], Wensheng Huang[2‡‡], James Myers[3§§], John Yim[2***], George Williams[4†††], Alejandro Lopez Ortega[1‡‡‡], Benjamin Jorns[1§§§], Michael Sekerak[1****], Christopher Griffiths[3††††], Rohit Shastry[2‡‡‡‡], Thomas Haag[2§§§§], Timothy Verhey[2*****], Bradley Gilliam[5†††††], Ira Katz[1‡‡‡‡‡], Dan Goebel[1§§§§§], John R. Anderson[1******], James Gilland[4††††††], Lauren Clayman[2‡‡‡‡‡‡]

[1]Jet Propulsion Laboratory, California Institute of Technology, Pasadena, CA
[2]NASA Glenn Research Center, Cleveland, OH
[3] Vantage Partners LLC, Brook Park, OH
[4] Ohio Aerospace Institute, Cleveland, OH
[5] ZIN Technologies, Middleburg Heights, OH

---

[*] Ion Propulsion System (IPS) Thruster Lead and Senior Engineer
[†] IPS Thruster Deputy Lead
[‡] IPS Lead
[§] IPS Deputy Lead and Principal Engineer
[**] IPS Lead System Engineer and Senior Engineer
[††] IPS Modeling and Simulation Lead and Principal Engineer
[‡‡] IPS Thruster Diagnostics Lead
[§§] IPS Thermal Engineer and Senior Aerospace Engineer
[***] IPS Modeling and Simulation Engineer
[†††] IPS Thruster Wear Testing Lead
[‡‡‡] IPS Modeling and Simulation Engineer
[§§§] IPS Thruster Diagnostics Engineer
[****] IPS Thruster Engineer
[††††] IPS Thruster Mechanical Design Lead
[‡‡‡‡] IPS Thruster Diagnostics Engineer and Research Engineer
[§§§§] IPS Mechanical Engineer
[*****] IPS System Engineer and Cathode Lead and Aerospace Scientist
[†††††] IPS System Engineer
[‡‡‡‡‡] IPS Modeling and Simulation Engineer and Principal Engineer
[§§§§§] IPS Thruster Diagnostics and Cathode Engineer and Senior Research Scientist
[******] IPS Thruster Engineer and Senior Engineer
[††††††] IPS Modeling and Simulation Engineer and Senior Scientist
[‡‡‡‡‡‡] IPS Thermal Engineer and Mechanical Engineer

The Hall Effect Rocket with Magnetic Shielding (HERMeS) is a 12.5 kW Hall thruster being co-developed by NASA Glenn Research Center and the Jet Propulsion Laboratory for the Space Technology Mission Directorate's Solar Electric Propulsion Technology Demonstration Mission. HERMeS incorporates technologies developed by NASA over nearly two decades, and is enabled through the use of magnetic shielding to effectively eliminate discharge chamber erosion. The result is a significant increase in the Hall thruster state-of-the-art, with HERMeS being designed to operate at 3000 s specific impulse and a lifetime of 50 kh. These capabilities are expected to meet or exceed the requirements for the proposed Asteroid Redirect Robotic Mission, which will utilize a 40 kW propulsion system with up to three HERMeS thrusters firing simultaneously. The thruster specification is described in terms of this system. A development approach was formulated from a set of technical risks including life qualification, facility effects, and spacecraft accommodation. The unique challenges of addressing these areas for magnetically shielded, high-power Hall thrusters are described. The thruster resulting from this approach includes an integrated magnetic and thermal design, pole piece covers, a graphite cathode keeper, an internally mounted cathode, and a downstream-plenum gas distributor. The completion of the first HERMeS test campaign has demonstrated magnetically shielded operation at high specific impulse. Testing has also verified that the internally mounted cathode minimizes the effects of facility pressure on performance and that, as expected, magnetic shielding is not affected by changes in facility pressure. On-going development activities are described.

I. Introduction

THE sustained exploration by humans of the inner solar system will require advances in multiple areas spanning nearly every aspect of space technology [1-3]. In-space power and propulsion, such as the high-power solar arrays and electric thrusters now being developed by the NASA Space Technology Mission Directorate (STMD) Solar Electric Propulsion Technology Demonstration Mission (SEP TDM), are among these technologies [4]. As part of the electric thruster development, the Hall Effect Rocket with Magnetic Shielding (HERMeS) is being co-developed by NASA Glenn Research Center (GRC) and the Jet Propulsion Laboratory (JPL) [5]. Shown in Figure 1, this 12.5 kW Hall thruster is being designed to be capable of operating at 3000 s specific impulse with a service life of 50 kh.

These capabilities are expected to meet or exceed the requirements for the proposed Asteroid Redirect Robotic Mission (ARRM), a mission under development by NASA to visit a large near-Earth asteroid, collect a multi-ton boulder from its surface and redirect it into a stable orbit around the moon [6-12]. ARRM will carry up to 10,000 kg of xenon for use in its 40 kW SEP system, which constitutes a significant extension over the demonstrated capabilities of any SEP technology. For example, this total propellant load is 24 times greater than the 425 kg launched on the Dawn mission, the largest xenon propellant load launched to date.

Hall thrusters are now expected to meet or exceed such extraordinary throughput requirements due to the recent breakthrough advances enabled by magnetic shielding [13-17]. Magnetic shielding physics were first identified through numerical simulation of Aerojet Rocketdyne's XR-5 Hall thruster [13,14] and subsequently validated through simulations and experiments that modified the unshielded (US) H6 Hall thruster for magnetic shielding (MS) and then renamed the H6MS [16-18]. Further, the recent demonstration of magnetic shielding at 3000 s specific impulse with the H6MS [19,20] and to high-power at 20 kW with the NASA-300MS [21-23], have achieved the long-held goal of NASA Hall thruster research of achieving long-life together with high specific impulse and high power. Additional investigations have demonstrated the extension of magnetic shielding to conducting wall thrusters [24] and low-power [25]. These capabilities are important milestones since they extend the application of Hall thrusters to the vast majority of robotic and human missions that NASA is likely to pursue for the next several decades.

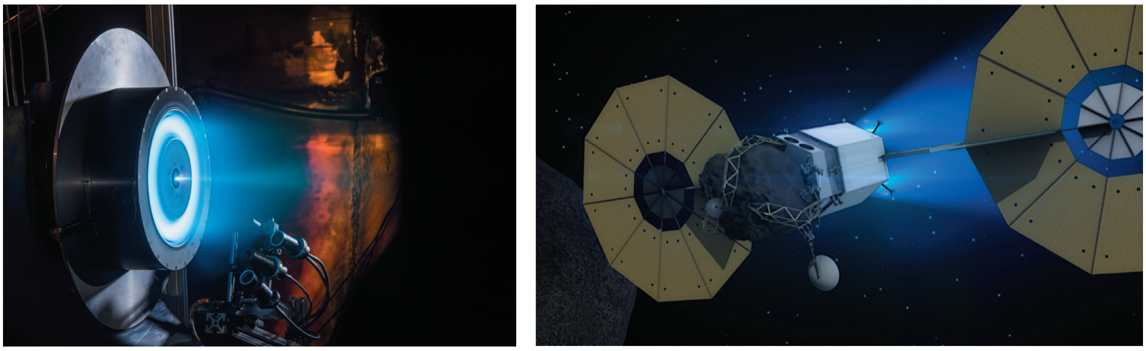

Figure 1. Left: HERMeS is a 12.5 kW Hall thruster capable of operation up to 3000 s specific impulse with a service life of 50 kh. Right: NASA is developing ARRM, a proposed robotic mission that would be the first to visit a large near-Earth asteroid, collect a multi-ton boulder from its surface, and redirect it into a stable orbit around the moon. ARRM is part of NASA's plan to advance the new technologies needed for human missions to Mars, and will require long-life, high-power Hall thrusters operating at up to 3000 s specific impulse.

HERMeS is the first Hall thruster designed for magnetic shielding over its entire service life [5]. In order to realize long-lifetime at high specific impulse, HERMeS brings together advances in thruster performance and lifetime from NASA Hall thruster research since the turn of the century [15-17,19,20,22,26-34]. The development of several key design tools has progressively improved performance and hardware fidelity and now includes a full suite of physics-based software models of the magnetic circuit, anode/gas distributor, cathode, discharge chamber plasma, and plume, alongside standard engineering tools modeling the mechanical design, structural dynamics, and thermal design. To achieve its design goals HERMeS uses an integrated magnetic and thermal design, pole piece covers, a graphite cathode keeper, an internally mounted cathode, and a downstream-plenum gas distributor.

In this paper, we describe the development approach and status of HERMeS. A comprehensive overview previously reported by Kamhawi, et al. [5], as well as a multitude of related papers [35-54], provide additional detail on topics not covered here. In the next section, the thruster specification is described followed by a description of the development approach and design features of the thruster. Key results from recent testing of the first HERMeS thruster are then described that have demonstrated magnetically shielded operation at high specific impulse and verified that the internally mounted cathode minimizes the effects of facility pressure on performance. We conclude with a discussion of the on-going development activities aimed at reducing risk prior to the next phase of HERMeS development.

II. Design Specification

The HERMeS design specification is derived from the key requirements for the ARRM Ion Propulsion System (IPS) listed in Table 1. The ARRM IPS must be capable of: operating at 3000 s specific impulse, processing 10,000 kg of xenon propellant, operating over a solar range of 0.8-1.9 AU, and operating at an input power up to 40 kW. The input power is divided equally across N active thrusters with single fault tolerance at the string level (i.e., an N+1 system). The system mass and cost model described in Ref. [55] was used to show that individual power thruster levels of 8-40 kW are within 10% of the system optimum. The relative flatness of the cost curves near the optimum allows for a selection of the power per thruster based on other factors, such as

- Designs with demonstrated performance and life technologies (e.g., 6 kW H6MS and 20 kW NASA-300MS)
- Fallback options for meeting life requirements (easier to double up smaller thrusters)
- Ease of testing and ground-test facility limitations (favors smaller thrusters)
- Manufacturability (favors smaller thrusters)
- Time constraints that may limit how many thrusters can complete acceptance testing on time (favors larger thrusters)
- If thruster life limits require carrying extra strings to meet the total mission impulse requirements, the total number of thrusters that must make it through acceptance testing before launch must be considered (favors larger thrusters)
- Extensibility to future missions in human spaceflight (favors larger thrusters), science missions (smaller), and the commercial marketplace (smaller)

With these considerations, other inputs from stakeholders, and the assumption of a 94% efficient power processing unit (PPU), a 12.5 kW discharge power (13.3 kW PPU input power) was selected for a 3+1 string architecture.

Table 2 lists some of the design attributes of a single HERMeS thruster derived from the ARRM IPS requirements. A Hall thruster producing 3000 s specific impulse requires a discharge voltage of about 800 V. The 50 kh service life is found by using the flow rate to current ratio of the H6MS operating at 800 V, 9 kW and a cathode flow fraction of 7% [19]. The minimum discharge power falls out after considering the maximum solar range (1.9 AU) and the power throttling characteristics of the three string system shown in Figure 2. Here it is assumed that the available power is split evenly across the thrusters and that thrusters are turned off when it is possible to run at a higher power per thruster. At the maximum solar range of 1.9 AU, the system still has 11.1 kW of power, but the minimum power per thruster actually occurs when the system power is just above 13.3 kW, or approximately 6.7 kW per thruster (i.e., 50% of maximum power per thruster). Thus, the power throttling ratio for this system is 2:1. It is also interesting to note that, 1) two thrusters are operating at >50% maximum power at the maximum Mars solar range (1.66 AU), and 2) the system could fly as far as 2.45 AU without dropping below 50% maximum power per thruster.

With the 50% power throttling needed by the ARRM IPS in Section II and additional considerations described in Ref. [38,40,53], the operating envelope of HERMeS can be specified. Figure 3 shows the resulting operating envelope of HERMeS and Table 3 lists the discrete operating points forming that envelope. The operating envelope spans 300-800 V discharge voltage, 8.9-31.3 A discharge current (3.5:1), and 6.25-12.5 kW discharge power. The relatively narrow 3.5:1 discharge current ratio is also beneficial for cathode lifetime.

The operating envelope of HERMeS shown in Figure 3 is by no means the full throttling capability of the thruster and, as might be needed for a science mission at large solar range, may be extended to power levels less than 6.25 kW at 700 V or less. Although the present development is not concerned with developing a thruster to these levels, HERMeS has been demonstrated in the laboratory to operate as low as 300 V, 0.6 kW. Figure 4 shows the operating conditions that have been investigated to date in the laboratory as discrete points overlaid on the operating envelope. If 0.6 kW operation were used with the ARRM IPS, the power throttling ratio would be 63:1 for a 3+1 system or, if operated as a single thruster, 21:1.

Table 1. **Key requirements of the ARRM IPS.**

Capability	Value
Total system power	40 kW
Maximum specific impulse	3000 s
Xenon throughput	10,000 kg
String fault tolerance	Single
Solar range	0.8 – 1.9 AU

Table 2. **Design attributes of a single HERMeS thruster derived from the ARRM IPS requirements.**

Attribute	Value
Maximum input power to PPU	13.3 kW
Maximum discharge power	12.5 kW
Discharge voltage at 3000 s I_{sp}	800 V
Discharge current at 3000 s I_{sp}	15.6 A
Service life (unmargined)	50,000 h
Minimum discharge power	6.25 kW (50% maximum power)

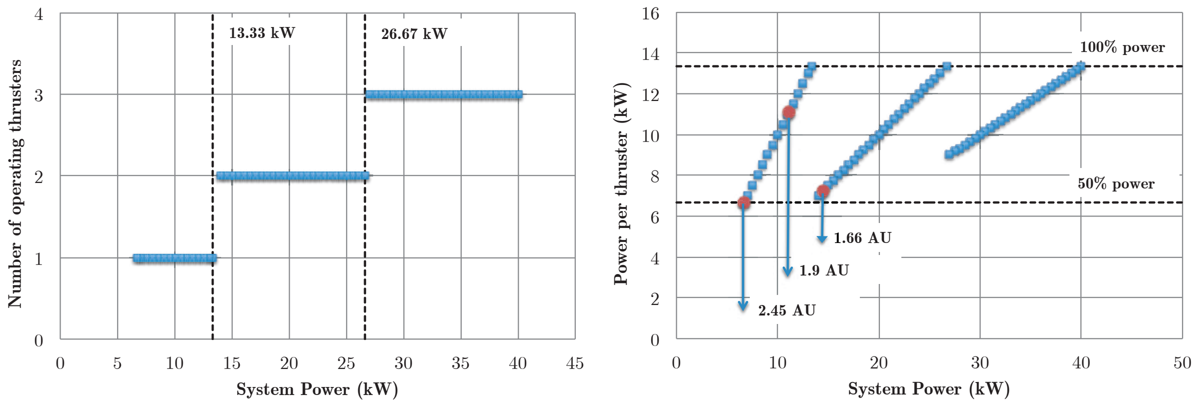

Figure 2. Number of operating thrusters (left) and power per thruster (right) of a 3+1 architecture as the total system power is varied. For this architecture, the minimum power per thruster is determined by the number of strings, not by the maximum solar range (1.9 AU). Also shown are the power per thruster at the maximum solar range of Mars (1.66 AU) and at the maximum solar range (2.45 AU) if an individual thruster is never throttled below 50% maximum power.

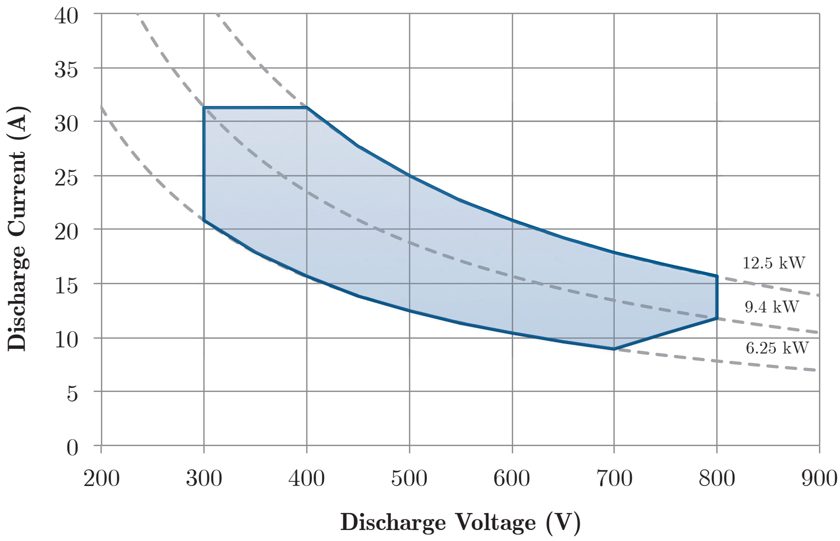

Figure 3. HERMeS operating envelope for the ARRM IPS.

Table 3. HERMeS operating conditions for the ARRM IPS.

Discharge Voltage (V)	Discharge Current (A)	Discharge Power (kW)
400	31.3	12.5
500	25.0	12.5
600	20.8	12.5
700	17.9	12.5
800	15.6	12.5
300	31.3	9.4
400	23.5	9.4
500	18.8	9.4
600	15.7	9.4
700	13.4	9.4
800	11.8	9.4
300	20.8	6.25
400	15.6	6.25
500	12.5	6.25
600	10.4	6.25
700	8.9	6.25

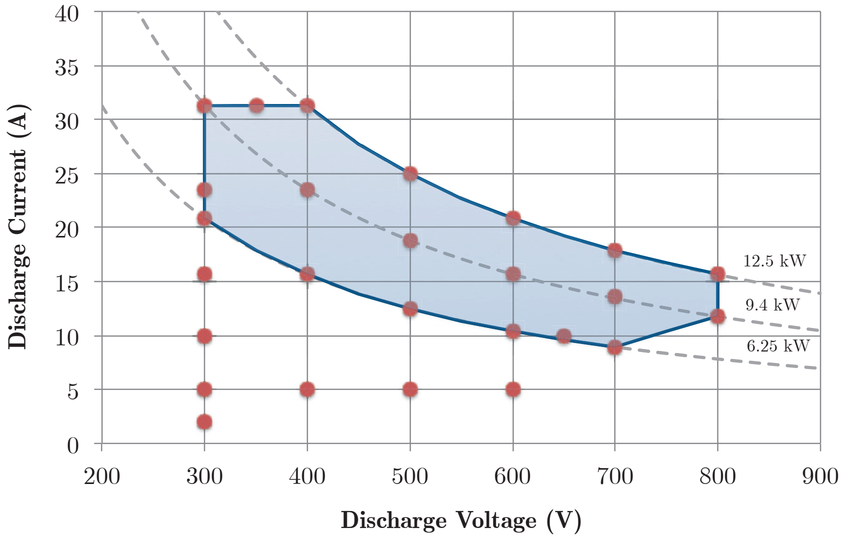

Figure 4. HERMeS operating envelope for the ARRM IPS (shaded region) and the discrete operating conditions demonstrated to date in the laboratory (red markers).

III. Development Approach and Design Features

The HERMeS development plan was formulated from a set of technical risks that could impact mission success. Each element of the development plan is traceable to these risks. The development consists of three major hardware build phases: the Technology Development Unit (TDU), Engineering Development Unit (EDU), and the combined Qualification Model (QM) and Flight Model (FM) phases. HERMeS is now in the TDU phase, which is scheduled to complete by mid-2016, and the project is on track to complete all of its planned tasks prior to the EDU phase starting. The risk areas most strongly driving the development plan include:

Life Qualification: The mission development schedule for ARRM precludes wear testing on the ground for the durations conventionally required. This necessarily means exceptions to the standard electric propulsion life qualification approach wherein 100% of the required impulse are demonstrated in wear testing and 50% margin is established by probabilistic risk analysis supported through physics-based modeling of the wear-out failure modes [56]. This deviation from the state-of-practice for HERMeS introduces a risk that the qualification approach will be insufficient and may require costly changes to the spacecraft (e.g., by adding thruster strings) or may reduce the propulsive capabilities of the spacecraft. To address these risks, an approach to certifying the life of HERMeS is being developed that relies on physics-based modeling and limited testing of the primary wear-out failure modes. The primary models being used are OrCa2D and Hall2De [17,57-59], which simulate the hollow cathode and thruster, respectively. The models are applied to discharge chamber erosion, pole piece erosion, and cathode wear-out failure modes. Both of these codes have been validated extensively in the past, but are being verified against results from HERMeS testing such as those in Ref. [47,48]. Additional detail of the life qualification plan is discussed in Section V.

Facility Effects: The performance, stability, thermal, and wear characteristics of all electric thrusters are influenced to some degree by the limitations of ground test facilities. Some of these limitations include finite operating pressures, volume constraints, the influence of grounded vacuum chamber walls, the thermal environment, and backsputter from the chamber walls. In recent years, the electric propulsion community has focused on the influence of ground test effects on flight performance, specifically with Hall thrusters. Since HERMeS is the first development of a high-power, magnetically shielded Hall thruster, there is the risk that the thruster design may be influenced differently by facility effects than prior electric thrusters. As a result, the development plan for HERMeS includes efforts to quantify facility effects and to develop designs or methodologies to mitigate them such that the performance and life of HERMeS may be reliably predicted during in-space operation.

Previous testing with the H6MS has demonstrated that magnetically shielded Hall thrusters using internally mounted cathodes are significantly less sensitive to pressure effects on stability and performance [60]. Recent HERMeS testing summarized in Section IV and described in detail by Kamhawi, et al in Ref. [40] have verified the H6MS results at lower backpressure. Additionally, methodologies described by Huang, et al in Ref. [61] that correct for pressure effects on plume measurements are being applied to HERMeS and are also described in Ref. [40]. Modeling of the vacuum chamber environment and the results from Hall2De simulations of the discharge chamber plasma using Hall2De are also being used to assess the impact of the chamber environment on thruster operation [52,60]. Collectively, the experimental results are establishing the methodologies necessary to account for facility effects and are indicating that HERMeS may in fact be less susceptible to facility effects than other thrusters [62]. Additional details are discussed in Section IV and V.

Spacecraft Accommodation: The high-energy plume of electric thrusters interacts with the spacecraft through sputtering of spacecraft surfaces, induced torques, and deposition on the spacecraft from thruster erosion products or re-deposition from sputtered spacecraft surfaces. Hall thrusters have been successfully integrated on many commercial spacecraft and a large body of knowledge exists describing ground testing, on-orbit measurements, and plume modeling. However, magnetically shielded Hall thrusters have larger plume divergence angles than unshielded thrusters and may have larger populations of primary ions at high angles. ARRM will also operate multiple thrusters simultaneously so any plume interactions affecting the operation of the thrusters and spacecraft surfaces must be understood and accounted for. To address these spacecraft accommodation risks, the development of HERMeS includes ground testing and plume modeling to assess these effects [40,50]. Additional details are discussed in Section IV and V.

The risks outlined above have informed the design of HERMeS throughout its development, resulting in design features that mitigate these risks. These include:

- A circular geometry using a single outer coil and a cathode mounted on thruster centerline that makes the thruster system axisymmetric. The symmetry provides accurate and efficient modeling of several aspects of the thruster, especially the cathode plume and associated electron transport [42-44].
- A monolithic boron nitride (BN) discharge chamber that is thermally coupled to an external radiator (Figure 7) in order to manage the interior temperatures of the thruster, especially the inner coil. Results from thermal testing are discussed further in Section IV and in Ref. [41].
- A magnetic circuit providing a magnetically shielded field topology and field strength margins before pole saturation. A high field strength capability was chosen so that the thruster would have adequate margins over its service life on orbit. The IPS is also being developed to provide independent control of the inner and outer electromagnets. Extensive testing has also been conducted in order to validate the magnetic circuit design software and magnetic field measurement technique that are being used (a portion of the code validation effort is described in Ref. [25]).
- Pole covers for the mitigation of erosion of the front pole pieces [19,42,47,63]. Pole erosion resulting from the field topology of magnetically shielded thrusters is still significantly lower than the erosion rates of channel walls in unshielded Hall thrusters, but if HERMeS is to meet the 50 kh service life goal, this issue must be addressed through identification of the physics involved and engineering solutions. A detailed modeling and experimental campaign is underway to address pole erosion. Spray-coated alumina is presently being used in testing to protect the pole

pieces, but graphite pole covers will be tested by the end of 2015. Additional details are provided in Section V.

- An innovative downstream-plenum gas distributor with backsputter protection [36,37].
- An internally mounted hollow cathode. It has been shown with the H6MS that Hall thrusters using internally mounted cathodes minimize the effects of finite facility background pressure on performance and stability, providing a path for reliably correlating ground tests with flight performance [17]. As described further in Section IV, testing with HERMeS have confirmed the previous H6MS results [40].
- A pair of hollow cathode technologies, both utilizing graphite keepers, are being developed and are described further in Section V. The first uses a barium oxide (BaO) impregnated porous tungsten emitter while the second uses a lanthanum hexaboride (LaB_6) emitter [5,45]. The IPS is being developed with the capability to meter the anode and cathode flow rates and provide for independent control of the cathode flow fraction.
- High-voltage gaps designed for backsputter resistance during wear tests that may require multiple chamber openings.
- High emissivity coatings for radiative heat rejection that are resistant to their thermal properties being significantly changed due to backsputtered carbon. Thermal interface materials are also being considered for part interfaces internal to the thruster where heat conduction is critical.

IV. Recent Results

HERMeS Technology Demonstration Unit 1 (TDU-1) has been fabricated and has recently completed the first test campaign of its performance, stability, thermal, and wear characteristics. A second thruster, TDU-2, is being fabricated that will undergo environmental testing by the end of 2015. TDU-1 testing has confirmed that the thruster is magnetically shielded at high specific impulse and that the cathode mounted on thruster centerline makes the design resilient against facility pressure effects.

An extensive array of diagnostics have been used in characterizing the TDU-1 thruster including [40]:

- Thrust stand
- Discharge current and voltage probes (time-resolved)
- High-speed camera
- Thermocouples and infrared camera
- Plume measurements using a Faraday probe, Langmuir probe, Retarding Potential Analyzer (RPA), and Wien filter spectrometer (WFS)
- Optical emission spectroscopy
- Discharge chamber wall probes
- Quartz crystal microbalance (QCM) and witness plates
- Ionization gauges mounted in various locations around the thruster

Major TDU-1 thruster characterizations have included:

- Performance and plume mapping spanning 0.6-13 kW and 300-800 V, including the effects of cathode flow fraction, magnetic field strength, and magnetic field symmetry [38,40]. Figure 5 shows performance corresponding to the conditions listed in Table 3 as well as operation as low as 300 V, 0.6 kW. Measurements of the flux, energy, and charge state of the ions in the plume are also being used to quantify facility effects and support spacecraft accommodation studies (see Section V).
- Impedance maps characterizing the discharge stability margins as a function of magnetic field strength [38].
- Multiple thermal characterizations with different hardware configurations that have quantified thermal margins [41,49]. The final configuration of TDU-1 includes an external radiator that is shown in Figure 7. The need for the radiator is described in Figure 8, which shows the discharge

chamber temperature versus the fraction of the discharge power that is radiatively rejected. To maintain discharge chamber temperatures less than 600 C, if the plasma power deposition is ~10% of the discharge power, approximately 3.5% of the discharge power (440 W) must also be rejected from other external surfaces. The surface area of the external surfaces is not large enough to support this amount of heat rejection with margin, so a radiator is used. With the radiator, HERMeS is able to maintain an average wall temperature of 530 C under worse case operating conditions (800 V, 12.5 kW, Maximum magnetic field strength) [40,41,49]. Figure 9 shows results from the HERMeS thermal model in Ref. [41] correlated to the same operating condition. Hall2De simulations have played an integral part in the thermal design process, by providing the incident plasma power to the thruster walls in the thermal model. Observed trends in the thermal response of the thruster during thruster testing with varying applied magnetic field (at constant power) are reproduced by the simulations. The trends are discussed in the context of the plasma evolution at the highest power, highest discharge voltage operating condition of 12.5 kW and 800 V in Ref. [44].

- Facility effects characterizations of the stability, thermal, performance, and wear [38,40,48]. Figure 6 shows results from a constant power evaluation of HERMeS TDU-1 at backpressures as low as 4 uTorr in VF5 at NASA GRC [38,40]. Consistent with previous investigations of the H6MS [60], performance is resilient against facility pressure effects due to the use of an internally mounted cathode.
- Wall probe measurements verifying that the plasma conditions at the wall are consistent with those necessary for magnetic shielding (Figure 10 and Table 4) [48]. Additionally, wall probe measurements taken over a factor of three in facility pressure at 300 V, 9.4 kW have demonstrated, as expected, that the plasma properties at the wall are constant (not shown, see Ref. [48]).

Additional results from these and related test campaigns and modeling activities are being presented this summer at various conferences and in future publications [35-54].

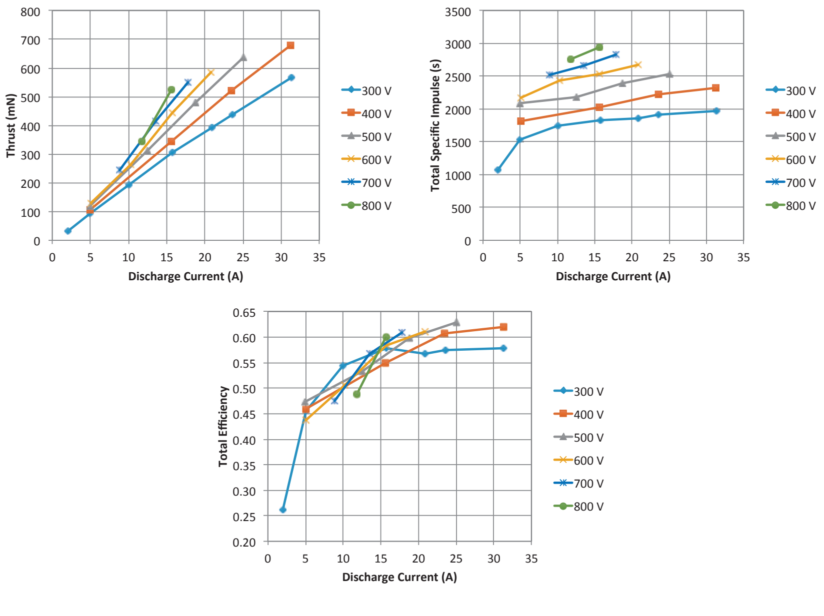

Figure 5. Thrust, specific impulse, and efficiency of HERMeS TDU-1 from May 2015 testing in VF5 at NASA GRC [38,40].

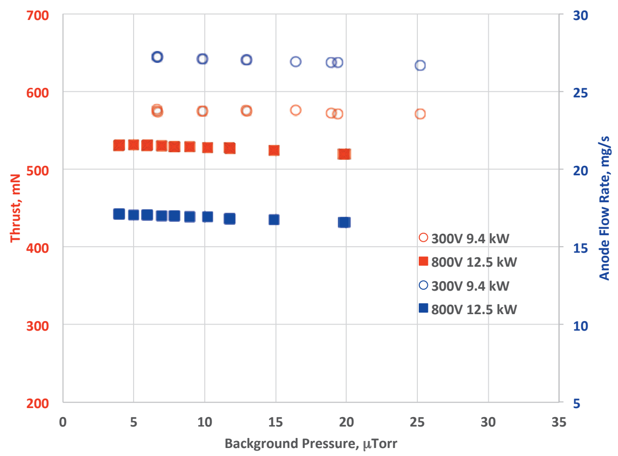

Figure 6. Constant power evaluation of HERMeS TDU-1 in VF5 at NASA GRC [40]. Consistent with previous investigations of the H6MS [60], the internal cathode configuration provides for a design resilient to facility effects.

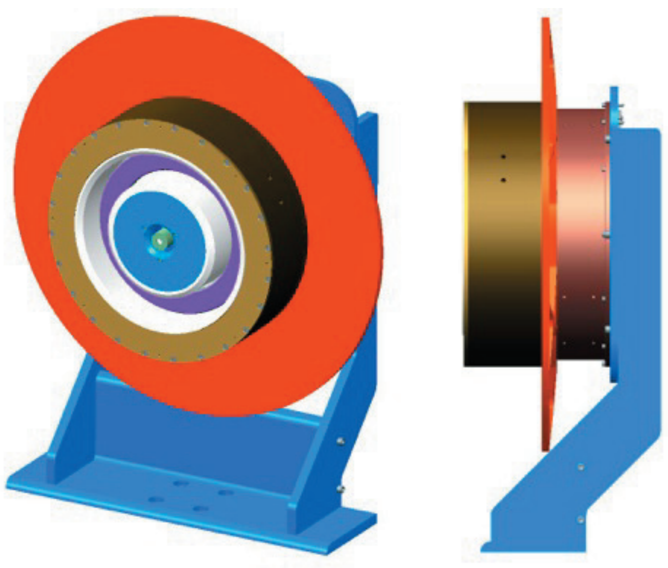

Figure 7. Solid model of HERMeS TDU-1 showing the radiator (orange) used to manage internal component temperatures and the thrust stand mount used during testing. The aluminum radiator is attached to the back pole and extends to the radius of the inner screen of the magnetic circuit where the back pole is near its maximum temperature (not shown).

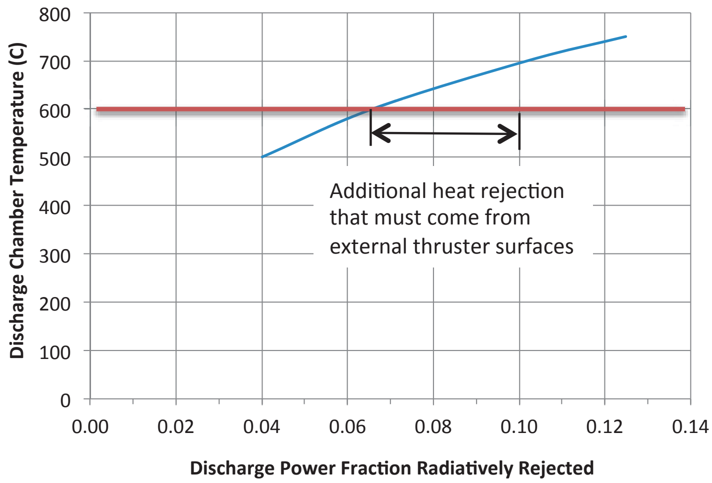

Figure 8. Discharge chamber temperature versus the fraction of the discharge power that is radiatively rejected. If the plasma power deposition is 10% of the discharge power, in order to maintain a 600 C discharge chamber temperature, approximately 3.5% of the discharge power (440 W) must also be rejected from other external surfaces. The surface area of these components is not large enough to support this amount of heat rejection with margin, so a radiator is used. With the radiator, HERMeS is able to maintain an average wall temperature of 530 C under worse case operating conditions (800 V, 12.5 kW, maximum magnetic field strength).

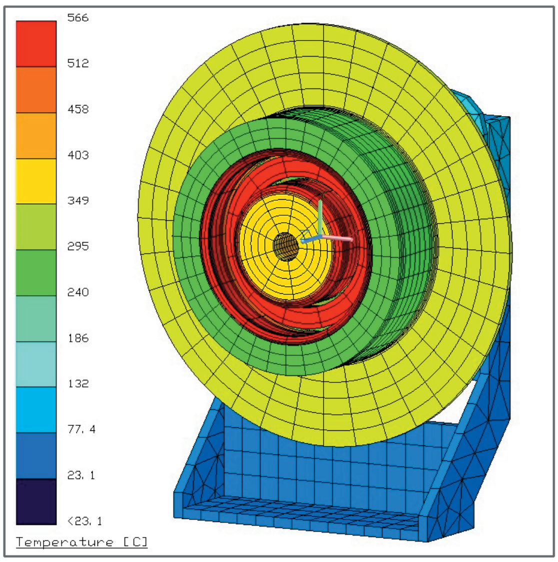

Figure 9. Results from the HERMeS thermal model correlated under the worse case operating condition for the thruster at 800 V, 12.5 kW and maximum magnetic field strength [41]. The agreement with experimental data is better than 20 C.

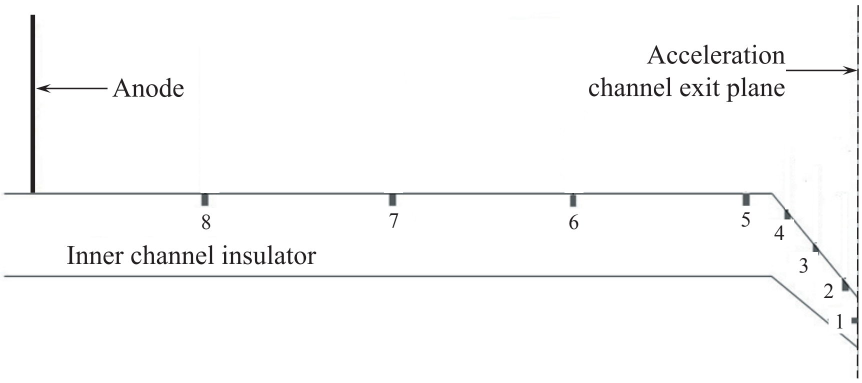

Figure 10. Axial location of the wall probes installed along the inner channel wall of HERMeS TDU-1 during the magnetic shielding characterization test [48]. Identical probe locations were used along the outer wall.

Table 4. Comparison of the plasma potential (with respect to the cathode) and electron temperature from Ref. [48] measured by wall probes 2 and 5 imbedded in the channel walls (see Figure 10) with those from the numerical simulations in Ref. [44]. The operating conditions are 300 V, 9.4 kW, and 800 V, 12.5 kW. As detailed in Ref. [48], the plasma conditions necessary for magnetic shielding were confirmed in HERMeS.

Operating Condition	Probe 2								Probe 5							
	Inner Wall				Outer Wall				Inner Wall				Outer Wall			
	ϕ_{pE}	ϕ_{pS}	T_{eE}	T_{eS}	ϕ_{pE}	ϕ_{pS}	T_{eE}	T_{eS}	ϕ_{pE}	ϕ_{pS}	T_{eE}	T_{eS}	ϕ_{pE}	ϕ_{pS}	T_{eE}	T_{eS}
9.4 kW	306	301	3	1.1	308	302	5	1.1	307	307	3	1.8	307	306	3	1.5
12.5 kW	809	805	3	1.1	808	805	4	1.1	NA	808	NA	1.8	807	808	3	1.6

V. Development Activities

HERMeS development activities are on-going with a focus on reducing risk prior to the start of the EDU development phase. These activities will extend in to the EDU and QM/FM phases of HERMeS, in particular in the areas of life qualification, facility effects, and spacecraft accommodation. Specific activities being worked prior to the EDU phase of development starting include the following:

TDU-1 data analysis: A large data set was acquired during the November 2014 – May 2015 test campaign covering the performance, stability, thermal, and wear characteristics of TDU-1 [38,40,48,49]. These data will be used to define margins related to stability, temperature, magnetic field, and wear as well as to define corrections for facility effects, the refinement of throttle curves for trajectory analysis, and plume analysis for spacecraft accommodation studies.

TDU-2 fabrication and environmental testing: A second TDU is being fabricated that incorporates the thermal design updates from TDU-1 [41] and advances the structural design prior to environmental testing at JPL scheduled for the Fall of 2015. Environmental testing for the expected launch and deep-space environments will include vibration and thermal cycling, similar to the campaign described in Ref. [64].

Cathode development: The development and evaluation of candidate BaO and LaB_6 hollow cathode technologies is in progress [5,45,46] with a down select planned prior to the start of the EDU phase. BaO cathodes have extensive heritage in US electric thrusters and are more capable of throttling to low currents [13,65], but LaB_6 cathodes are more resistant to propellant impurities and more extensible to high-current operation [66-68]. Insert temperature and impurity resistance experiments will be executed this summer for both cathodes. A high-temperature heater qualification is starting for the LaB_6 cathode and both cathodes will undergo wear testing this year. Modeling using OrCa2D [57,58] to predict keeper erosion, cathode orifice erosion, and insert life are underway for both cathodes. A common brazed design is also in development that will include vibration testing to verify the design.

Spacecraft accommodation: Plume data and plasma simulations from TDU-1 are being used to characterize how energetic ions interact with the spacecraft. The plume data from TDU-1 is being used to validate a Hall2De-based plume model in the vacuum chamber environment [40,50]. Once validated, the models will be applied to the spacecraft environment so that interactions of the thruster plumes with the spacecraft may be assessed. Multi-thruster operation is also being considered as ARRM will operate up to three thrusters simultaneously, a first for the use of electric thrusters on a NASA mission.

Life qualification: Magnetic shielding essentially eliminates discharge chamber erosion as the primary failure mode in Hall thrusters. This greatly extends the service life of Hall thrusters, but other components are subject to wear out failure modes that also must be accounted for. Among these include pole erosion, several cathode failure modes (insert depletion, keeper erosion, cathode orifice erosion, heater failure), electromagnet insulation failures, and other failure modes related to high-temperature operation and thermal cycling (e.g., propellant isolator or anode structural failures). None of these secondary modes are expected to limit the service life to less than 50 kh. Whenever possible, physics-based models are being developed for each failure mode that are validated through testing (see Section III).

The development of a detailed life qualification plan and validation effort is currently in progress. The 50 kh service life will preclude the possibility of a wear test demonstrating 100% of the required impulse prior to the projected launch on the proposed ARRM mission, so it will be a practical necessity to use physics-based modeling combined with limited wear testing in the life certification of HERMeS [69]. A major element of this plan is wear testing of the thruster and cathodes, which is planned to include a series of progressively longer tests. A 2 kh wear test of TDU-1 is planned for late 2015, which will be the longest wear test to date of a NASA magnetically shielded thruster. The 2 kh wear tests is a pathfinder aimed at addressing specific challenges of wear testing magnetically shielded thrusters, monitoring the long term performance, and potentially identifying previously unknown failure modes. Models of the vacuum chamber pumping system and distribution of backsputtered carbon are also being developed to aid in designing this wear test. Additional wear testing and modeling is being conducted with the H6MS and with TDU-2 in the development of techniques to address pole erosion. In particular, a 500 h wear test is planned with TDU-2 for the final pole cover design, which may not be finalized prior to the 2 kh wear test of TDU-1.

Magnetic shielding also creates a new complication in qualifying Hall thrusters due to the build-up of backsputtered carbon from the vacuum facility on the discharge chamber walls of the thruster. As the carbon films become thicker over time, the long term behavior of the thruster may change. Wear testing conducted with the H6MS has suggested that the thruster will begin to operate much like the walls were made from carbon, as it has been observed that the performance of the H6MS has approached that of the H6C (carbon wall) within the first 100 h of testing [24,47]. Since backsputtered carbon is a practical reality of wear testing on the ground, it is natural to ask whether the wall material should instead be changed to carbon. This approach would eliminate the potential test-as-you-fly exception that the carbon films create, but would have the added complication of designing a conducting channel that could maintain high-voltage isolation over thousands of hours of operation. The HERMeS team is considering evaluating a graphite discharge chamber assembly in HERMeS by mid-2016 as an approach to eliminate the test-as-you-fly exemption. This benefit is being weighed against potential conducting wall channel disadvantages.

The long-term impact of non-uniform gas distribution and the effects of carbon films on the anode/gas distributor are also being investigated as part of the life qualification effort. It is well known that non-uniform flow can decrease performance and create regions of high temperature in the discharge chamber, and can even lead to plasma instabilities [70]. Much less is known about the impact of non-uniform flow on thruster life. It may be sufficient that the flow simply needs to be uniform enough to not cause measurable impacts on the performance, thermal, and stability characteristics. However, the life for HERMeS is five times longer than previous test experience, so the possibility of non-uniform flow impacting the long-term behavior of the thruster can not be excluded. To address these issues, gas distributors are being developed with high levels of uniformity as are high-resolution neutral flow measurement diagnostics [36,37]. Gas distributors that are resistant to the effects of backsputtered carbon during wear tests are also being investigated.

Magnetic shielding requires a much higher level of control of the magnetic field topology in the discharge chamber than unshielded thrusters. While magnetic field simulation software may be used to accurately design the pole pieces, the translation of such models to a working device requires a detailed understanding of the magnetic properties of the materials used, the heat treatment and fabrication processes necessary to achieve the desired magnetic performance, the mechanical and thermal designs that will maintain the field topology over the thruster life, and the diagnostic methods to accurately measure the magnetic fields. Investigations in these areas are on-going, with a focus on defining the magnetic field margins in as-built hardware and the impact of these margins on thruster life.

Materials: Testing of several thruster materials are currently underway and new materials are being considered for some thruster components such as the pole piece covers. The focus of these investigations are materials such as the ceramics used in the discharge chamber, magnetic materials, low-sputtering materials, and high-temperature materials.

High-temperature coils: A limiting factor in the thermal design of the thruster is the temperature of the inner magnetic circuit, in particular the inner electromagnet. Detailed thermal models of the windings are being developed in conjunction with test coils that are instrumented with thermocouples and tested in controlled environments that include thermal cycling [41]. The results from these tests and simulations will be used to better define the thermal margins and life of the coil assemblies. Investigations of high-temperature coil materials are underway that may include the qualification of new assemblies if suitable alternatives are identified.

VI. Conclusion

HERMeS is a 12.5 kW Hall thruster designed for operation at 3000 s specific impulse and a 50 kh lifetime that is enabled through the use of magnetic shielding and multiple physics-based models of the magnetic circuit, plasma, thermal response, and neutral gas flow. The validation of these models is critical to the thruster life qualification that is to follow since a full wear test will not be accomplished prior to launch of the proposed ARRM mission. A development approach has been formulated to address the constraints of the mission timeline as well as specific aspects of magnetically shielded, high-power Hall thrusters. The major areas include life qualification, facility effects, and spacecraft accommodation. Testing of the first HERMeS thruster has verified that magnetic shielding is achieved at high specific impulse and that the thruster is resilient against facility pressure effects due to the use of an internally mounted cathode. Significant progress has been made in each development area and the project is on track to complete major risk reduction efforts prior to the EDU phase.

Acknowledgments

The support of the joint NASA GRC and JPL development of HERMeS by NASA's Space Technology Mission Directorate through the Solar Electric Propulsion Technology Demonstration Mission (SEP TDM) project is gratefully acknowledged. Portions of the research described in this paper were carried out at the Jet Propulsion Laboratory, California Institute of Technology, under a contract with the National Aeronautics and Space Administration. Thanks also to Ryan Conversano and Sean Reilly for their support with magnetic field and thermal modeling, respectively, and to John Brophy, David Manzella, David Jacobson, Robert Jankovsky, and Tom Randolph for providing their expertise and technical guidance to the development of HERMeS.

References

[1] Strange, N., Landau, D., Polk, J., Brophy, J., and Mueller, J., "Solar Electric Propulsion for a Flexible Path of Human Space Exploration," Presented at the 61st International Astronautical Congress, IAC-10.A5.2.4, Prague, Czech Republic, Sep.-Oct., 2010.

[2] Brophy, J., Gershman, R., Strange, N., Landau, D. F., Merrill, R., and Kerslake, T., "300-kW Solar Electric Propulsion System Configuration for Human Exploration of near-Earth Asteroids," AIAA Paper 2011-5514, 2011.

[3] Manzella, D. and Hack, K., "High-Power Solar Electric Propulsion for Future NASA Missions," AIAA Paper 2014-3718, July 2014.

[4] Mcguire, M. L., Hack, K. J., Manzella, D. H., and Herman, D. A., "Concept Designs for NASA's Solar Electric Propulsion Technology Demonstration Mission," AIAA Paper 2014-3717, July 2014.

[5] Kamhawi, H., Huang, W., Haag, T., Yim, J., Chang, L., Clayman, L., Herman, D. A., Shastry, R., Thomas, R., Griffith, C., Myers, J., Williams, G., Mikellides, I. G., Hofer, R. R. et al., "Overview of the Development of the Solar Electric Propulsion Technology Demonstration Mission 12.5-kW Hall Thruster," AIAA Paper 2014-3898, July 2014.

[6] Brophy, J. R., Gershman, R., Landau, D., Polk, J., Porter, C., Yeomans, D., Allen, C., Williams, W., and Asphaug, E., "Asteroid Return Mission Feasibility Study," AIAA Paper 2011-5565, July 2011.

[7] Brophy, J. and Oleson, S., "Spacecraft Conceptual Design for Returning Entire near-Earth Asteroids," AIAA-2012-4067, July 2012.

[8] Brophy, J. R. and Muirhead, B., "Near-Earth Asteroid Retrieval Mission (Arm) Study," Presented at the 33rd International Electric Propulsion Conference, IEPC Paper 2013-082, Washington DC, Oct. 6-10, 2013.

[9] Strange, N., Landau, D., Mcelrath, T., Lantoine, G., Lam, T., Mcguire, M., Burke, L., Martini, M., and Dankanich, J., "Overview of Mission Design for NASA Asteroid Redirect Robotic Mission Concept," Presented at the 33rd International Electric Propulsion Conference, IEPC Paper 2013-321, Washington, DC, Oct 6-10, 2013.

[10] Brophy, J. R., "Technology for a Robotic Asteroid Redirect Mission," Presented at the IEEE Aerospace Conference, 10.1109/AERO.2014.6836392, Big Sky, MT, Mar 1-8, 2014.

[11] Mazanek, D. D., Merrill, R. G., Belbin, S. P., Reeves, D. M., Earle, K. D., Naasz, B. J., and Abell, P. A., "Asteroid Redirect Robotic Mission: Robotic Boulder Capture Option Overview," AIAA Paper 2014-4432, Aug 2014.

[12] Muirhead, B. K. and Brophy, J. R., "Asteroid Redirect Robotic Mission Feasibility Study," Presented at the IEEE Aerospace Conference, 10.1109/AERO.2014.6836358, Big Sky, MT, Mar 1-8, 2014.

[13] De Grys, K. H., Mathers, A., Welander, B., and Khayms, V., "Demonstration of 10,400 Hours of Operation on 4.5 kW Qualification Model Hall Thruster," AIAA Paper 2010-6698, July 2010.

[14] Mikellides, I. G., Katz, I., Hofer, R. R., Goebel, D. M., De Grys, K. H., and Mathers, A., "Magnetic Shielding of the Acceleration Channel in a Long-Life Hall Thruster," Physics of Plasmas 18, 033501 (2011).

[15] Mikellides, I. G., Katz, I., Hofer, R. R., and Goebel, D. M., "Magnetic Shielding of Walls from the Unmagnetized Ion Beam in a Hall Thruster," Applied Physics Letters 102, 2, 023509 (2013).

[16] Hofer, R. R., Goebel, D. M., Mikellides, I. G., and Katz, I., "Magnetic Shielding of a Laboratory Hall Thruster Part II: Experiments," Journal of Applied Physics 115, 043303 (2014).

[17] Mikellides, I. G., Katz, I., Hofer, R. R., and Goebel, D. M., "Magnetic Shielding of a Laboratory Hall Thruster Part I: Theory and Validation," Journal of Applied Physics 115, 043303 (2014).

[18] Hofer, R. R., Goebel, D. M., Mikellides, I. G., and Katz, I., "Design of a Laboratory Hall Thruster with Magnetically Shielded Channel Walls, Phase II: Experiments," AIAA-2012-3788, July 2012.

[19] Hofer, R. R., Jorns, B. A., Polk, J. E., Mikellides, I. G., and Snyder, J. S., "Wear Test of a Magnetically Shielded Hall Thruster at 3000 Seconds Specific Impulse," Presented at the 33rd International Electric Propulsion Conference, IEPC-2013-033, Washington, DC, Oct 6-10, 2013.

[20] Mikellides, I. G., Hofer, R. R., Katz, I., and Goebel, D. M., "Magnetic Shielding of Hall Thrusters at High Discharge Voltages," Journal of Applied Physics 116, 5, 053302 (2014).

[21] Huang, W., Shastry, R., Soulas, G. C., and Kamhawi, H., "Farfield Plume Measurements and Analysis on the NASA-300m and NASA-300ms," Presented at the 33rd International Electric Propulsion Conference, IEPC Paper 2013-057, Washington, DC, Oct. 6-10, 2013.

[22] Kamhawi, H., Huang, W., Haag, T., Shastry, R., Soulas, G., Smith, T., Mikellides, I. G., and Hofer, R. R., "Performance and Thermal Characterization of the NASA-300ms 20 kW Hall Effect Thruster," Presented at the 33rd International Electric Propulsion Conference, IEPC-2013-444, Washington, DC, Oct 6-10, 2013.

[23] Shastry, R., Huang, W., Haag, T., and Kamhawi, H., "Langmuir Probe Measurements within the Discharge Channel of the 20-kW NASA-300m and NASA-300ms Hall Thrusters," Presented at the 33rd International Electric Propulsion Conference, IEPC Paper 2013-122, Washington, DC, Oct. 6-10, 2013.

[24] Goebel, D. M., Hofer, R. R., Mikellides, I. G., Katz, I., Polk, J. E., and Dotson, B. N., "Conducting Wall Hall Thrusters," IEEE Transactions on Plasma Science 43, 1, 118-126 (2015).

[25] Conversano, R. W., Goebel, D. M., Hofer, R. R., Mikellides, I. G., Katz, I., and Wirz, R. E., "Development and Validation Overview for the Design of Low Power Magnetically Shielded Hall Thrusters," Presented at the 62nd JANNAF Propulsion Meeting, JANNAF-2015-4173, Nashville, TN, June 1-5, 2015.

[26] Manzella, D. H., Jankovsky, R. S., and Hofer, R. R., "Laboratory Model 50 kW Hall Thruster," AIAA Paper 2002-3676, July 2002.

[27] Manzella, D. H., Jacobson, D. T., Peterson, P. Y., and Hofer, R. R., "Scaling Hall Thrusters to High Power," NASA Glenn Research Center, NASA/TM-2004-213087, May 2004.

[28] Hofer, R. R., Jankovsky, R. S., and Gallimore, A. D., "High-Specific Impulse Hall Thrusters, Part 1: Influence of Current Density and Magnetic Field," Journal of Propulsion and Power 22, 4, 721-731 (2006).

[29] Hofer, R. R. and Gallimore, A. D., "High-Specific Impulse Hall Thrusters, Part 2: Efficiency Analysis," Journal of Propulsion and Power 22, 4, 732-740 (2006).

[30] Haas, J. M., Hofer, R. R., Brown, D. L., Reid, B. M., and Gallimore, A. D., "Design of the H6 Hall Thruster for High Thrust/Power Investigation," Presented at the 54th JANNAF Propulsion Meeting, Denver, CO, May 14-17, 2007.

[31] Hofer, R. R., Johnson, L. K., Goebel, D. M., and Wirz, R. E., "Effects of Internally-Mounted Cathodes on Hall Thruster Plume Properties," IEEE Transactions on Plasma Science 36, 5, 2004-2014 (2008).

[32] Peterson, P. Y., Jacobson, D. T., Manzella, D. H., and John, J. W., "The Performance and Wear Characterization of a High-Power High-Isp NASA Hall Thruster," AIAA Paper 2005-4243, July 2005.

[33] Manzella, D. H., "Low Cost Electric Propulsion Thruster for Deep Space Robotic Science Missions," NASA Glenn Research Center, NASA/TM-2008-215067, March 2008.

[34] Kamhawi, H., Manzella, D., Pinero, L., and Haag, T., "In-Space Propulsion High Voltage Hall Accelerator Development Project Overview," Presented at the 57th JANNAF Propulsion Meeting, Colorado Springs, CO, May 3-7, 2010.

[35] Herman, D. A. and Unfried, K. G., "Xenon Acquisition Strategies for High-Power Electric Propulsion NASA Missions," Presented at the 62nd JANNAF Propulsion Meeting, JANNAF-2015-XXXX, Nashville, TN, June 1-5, 2015.

[36] Huang, W., Yim, J. T., and Kamhawi, H., "Design and Empirical Assessment of the HERMeS Hall Thruster Propellant Manifold," Presented at the 62nd JANNAF Propulsion Meeting, JANNAF-2015-XXXX, Nashville, TN, June 1-5, 2015.

[37] Yim, J. T. and Huang, W., "Flow Analysis and Modeling of the HERMeS Hall Thruster Propellant Manifold," Presented at the 62nd JANNAF Propulsion Meeting, JANNAF-2015-XXXX, Nashville, TN, June 1-5, 2015.

[38] Kamhawi, H., Haag, T., Huang, W., and Hofer, R. R., "The Voltage-Current Characteristics of the 12.5 kW Hall Effect Rocket with Magnetic Shielding at Different Background Pressure Conditions," Presented at the 62nd JANNAF Propulsion Meeting, JANNAF-2015-XXXX, Nashville, TN, June 1-5, 2015.

[39] Herman, D. A., Polk, J. E., Hofer, R. R., Santiago, W., Kamhawi, H., Scheidegger, R., and Pinero, L., "The Development of the Ion Propulsion System for the Solar Electric Propulsion Technology Demonstration Mission " Presented at the 34th International Electric Propulsion Conference, IEPC-2015-008, Kobe, Japan, July 4-10, 2015.

[40] Kamhawi, H., Haag, T., Huang, W., Herman, D. A., Thomas, R., Shastry, R., Yim, J., Chang, L., Clayman, L., Verhey, T., Griffiths, C., Myers, J., Williams, G., Mikellides, I. G. et al., "Performance Characterization of the Solar Electric Propulsion Technology Demonstration Mission 12.5-kW Hall Thruster," Presented at the 34th International Electric Propulsion Conference, IEPC-2015-007, Kobe, Japan, July 4-10, 2015.

[41] Myers, J., Kamhawi, H., and Yim, J., "HERMeS Thermal Model," AIAA-2015-XXXX, July 2015.

[42] Lopez Ortega, A., Mikellides, I. G., and Katz, I., "Hall2De Numerical Simulations for the Assessment of Pole Erosion in a Magnetically Shielded Hall Thruster," Presented at the 34th International Electric Propulsion Conference, IEPC-2015-249, Kobe, Japan, July 4-10, 2015.

[43] Katz, I., Mikellides, I. G., Jorns, B. A., and Lopez Ortega, A., "Hall2De Simulations with an Anomalous Transport Model Based on the Electron Cyclotron Drift Instability," Presented at the 34th International Electric Propulsion Conference, IEPC-2015-402, Kobe, Japan, July 4-10, 2015.

[44] Mikellides, I. G., Lopez Ortega, A., Hofer, R. R., Polk, J. E., Kamhawi, H., Yim, J. T., and Myers, J., "Hall2De Simulations of a 12.5-kW Magnetically Shielded Hall Thruster for the NASA Solar Electric Propulsion Technology Demonstration Mission," Presented at the 34th International Electric Propulsion Conference, IEPC-2015-254, Kobe, Japan, July 4-10, 2015.

[45] Goebel, D. M., Polk, J. E., Mikellides, I. G., and Lopez Ortega, A., "Lanthanum Hexaboride Hollow Cathode for the Asteroid Retrieval/Redirect Mission " Presented at the 34th International Electric Propulsion Conference, IEPC-2015-043, Kobe, Japan, July 4-10, 2015.

[46] Polk, J. E., Guerrero, P., Goebel, D. M., Mikellides, I. G., and Katz, I., "Thermal Characteristics of Lanthanum Hexaboride Hollow Cathodes," Presented at the 34th International Electric Propulsion Conference, IEPC-2015-044, Kobe, Japan, July 4-10, 2015.
[47] Sekerak, M., Hofer, R. R., Polk, J. E., Jorns, B. A., and Mikellides, I. G., "Wear Testing of a Magnetically Shielded Hall Thruster at 2000 S Specific Impulse," Presented at the 34th International Electric Propulsion Conference, IEPC-2015-155, Kobe, Japan, July 4-10, 2015.
[48] Shastry, R., Huang, W., and Kamhawi, H., "Near-Surface Plasma Characterization of the 12.5-kW NASA Tdu1 Hall Thruster," AIAA-2015-XXXX, July 2015.
[49] Huang, W., Kamhawi, H., Myers, J., Yim, J., and Neff, G., "Non-Contact Thermal Characterization of Nasa's 12.5-kW Hall Thruster," AIAA-2015-XXXX, July 2015.
[50] Lopez Ortega, A., Katz, I., Mikellides, I. G., and Goebel, D. M., "Self-Consistent Model of a High Power Hall Thruster Plume," Presented at the 13th Spacecraft Charging Technology Conference, Paper No. 124, Pasadena, CA, June, 2014.
[51] Williams, G. J. and Kamhawi, H., "Optical Characterization of Component Wear and near-Field Plasma of the HERMeS Thruster," Presented at the 62nd JANNAF Propulsion Meeting, Nashville, TN, June 1-5, 2015.
[52] Yim, J. T. and Burt, J. M., "Characterization of Vacuum Facility Background Gas through Simulation and Considerations for Electric Propulsion Ground Testing," AIAA-2015-XXXX, July 2015.
[53] Hofer, R. R., Kamhawi, H., Mikellides, I. G., Herman, D. A., Polk, J. E., Huang, W., Yim, J., Myers, J., and Shastry, R., "Design Methodology and Scaling of the 12.5 kW HERMeS Hall Thruster for the Solar Electric Propulsion Technology Demonstration Mission," Presented at the 62nd JANNAF Propulsion Meeting, JANNAF-2015-3946, Nashville, TN, June 1-5, 2015.
[54] Lopez Ortega, A. and Mikellides, I. G., "The Importance of the Cathode Plume and Its Interactions with the Ion Beam in Numerical Simulations of Hall Thrusters," Presented at the 34th International Electric Propulsion Conference, IEPC-2015-310, Kobe, Japan, July 4-10, 2015.
[55] Hofer, R. R. and Randolph, T. M., "Mass and Cost Model for Selecting Thruster Size in Electric Propulsion Systems," Journal of Propulsion and Power 29, 1, 166-177 (2013).
[56] Dankanich, J. W., Brophy, J. R., and Polk, J. E., "Lifetime Qualification Standard for Electric Thrusters," http://discovery.larc.nasa.gov/PDF_FILES/11_EP_Standard_Disc_Lib_final.pdf, AIAA-2009-5095, Aug. 2009.
[57] Mikellides, I. G., Katz, I., Goebel, D. M., Jameson, K. K., and Polk, J. E., "Wear Mechanisms in Electron Sources for Ion Propulsion, 2: Discharge Hollow Cathode," Journal of Propulsion and Power 24, 4, 866 (2008).
[58] Mikellides, I. G., Katz, I., Goebel, D. M., and Polk, J. E., "Hollow Cathode Theory and Experiment. II. A Two-Dimensional Theoretical Model of the Emitter Region," Journal of Applied Physics 98, 113303 (2005).
[59] Mikellides, I. G. and Katz, I., "Numerical Simulations of Hall-Effect Plasma Accelerators on a Magnetic-Field-Aligned Mesh," Physical Review E 86, 4, 046703 (2012).
[60] Hofer, R. R. and Anderson, J. R., "Finite Pressure Effects in Magnetically Shielded Hall Thrusters," AIAA Paper 2014-3709, July 2014.
[61] Huang, W., Kamhawi, H., and Haag, T., "Effect of Background Pressure on the Performance and Plume of the Hivhac Hall Thruster," Presented at the 33rd International Electric Propulsion Conference, IEPC Paper 2013-058, Washington, DC, Oct 6-10, 2013.
[62] Diamant, K. D., Liang, R., and Corey, R. L., "The Effect of Background Pressure on SPT-100 Hall Thruster Performance," AIAA Paper 2014-3710, July 2014.
[63] Goebel, D. M., Jorns, B., Hofer, R. R., Mikellides, I. G., and Katz, I., "Pole-Piece Interactions with the Plasma in a Magnetically Shielded Hall Thruster," AIAA Paper 2014-3899, July 2014.
[64] Snyder, J. S., Anderson, J. R., Van Noord, J. L., and Soulas, G. C., "Environmental Testing of Nasa's Evolutionary Xenon Thruster Prototype Model 1 Reworked Ion Engine," Journal of Propulsion and Power 25, 1, 94-104 (2009).
[65] Shastry, R., Herman, D. A., Soulas, G. C., and Patterson, M. J., "End-of-Test Performance and Wear Characterization of NASA's Evolutionary Xenon Thruster (Next) Long-Duration TestJuly 2014.
[66] Goebel, D. M. and Chu, E., "High-Current Lanthanum Hexaboride Hollow Cathode for High-Power Hall Thrusters," Journal of Propulsion and Power 30, 1, 35-40 (2014).
[67] Goebel, D. M. and Watkins, R. M., "Compact Lanthanum Hexaboride Hollow Cathode," Review of Scientific Instruments 81, 8, 083504 (2010).
[68] Goebel, D. M., Watkins, R. M., and Jameson, K. K., "LaB6 Hollow Cathodes for Ion and Hall Thrusters," Journal of Propulsion and Power 23, 3, 552-558 (2007).
[69] Brophy, J. R., Polk, J. E., Randolph, T. M., and Dankanich, J. W., "Lifetime Qualification of Electric Thrusters for Deep-Space Missions," AIAA Paper 2008-5184, July 2008.
[70] Hofer, R. R., "Development and Characterization of High-Efficiency, High-Specific Impulse Xenon Hall Thrusters," Ph.D. Dissertation, Aerospace Engineering, University of Michigan, Ann Arbor, MI, 2004. (Also NASA/CR-2004-213099)